FIG. 1

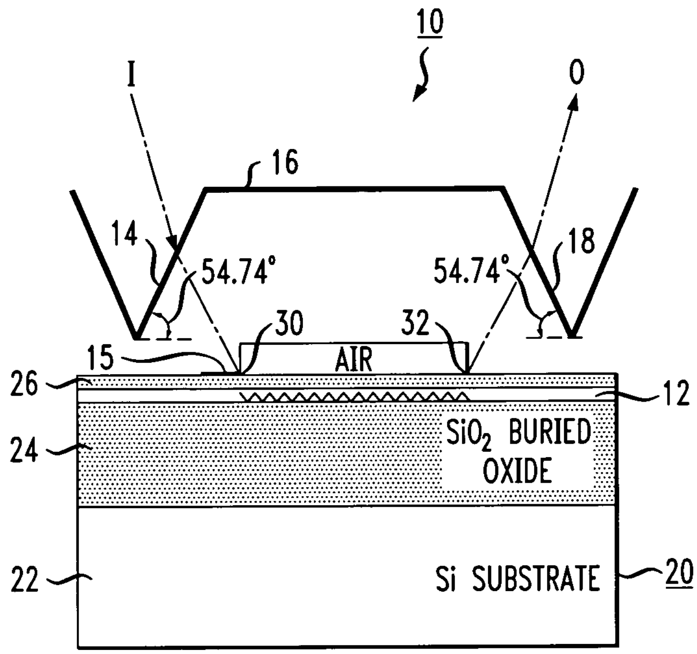
10
I
0
16
14
54.74°
54.74°
18
30
32
AIR
15
26
12
24
SiO_2 BURIED
OXIDE
22
Si SUBSTRATE
20

FIG. 2

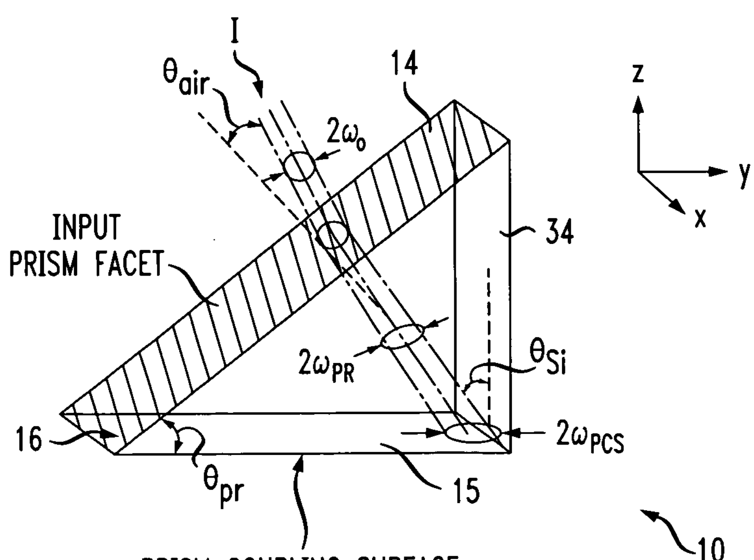
I
θ_{air}
14
z
y
x
$2\omega_o$
INPUT
PRISM FACET
34
$2\omega_{PR}$
θ_{Si}
16
$2\omega_{PCS}$
θ_{pr}
15
10
PRISM COUPLING SURFACE
(ADJACENT TO EVANESCENT COUPLING LAYER)

FIG. 3

WAVELENGTH DEPENDENCE OF BEAM ANGLE INSIDE PRISM (θ Si) AS A FUNCTION OF WAVELENGTH, FOR THREE DIFFERENT WAVEGUIDE THICKNESSES

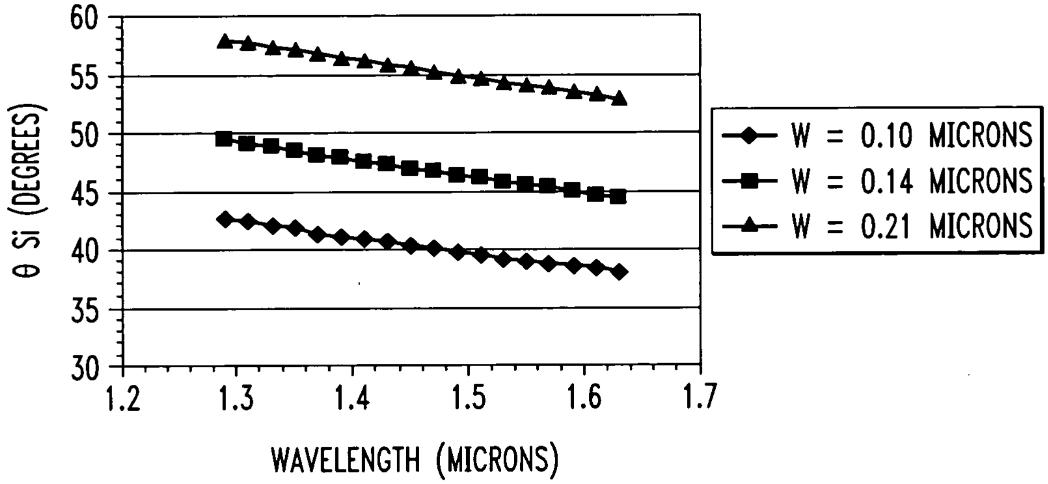

FIG. 4

WAVELENGTH DEPENDENCE OF BEAM ANGLE IN AIR (θ air) AS A FUNCTION OF WAVELENGTH, FOR THREE DIFFERENT WAVEGUIDE THICKNESSES

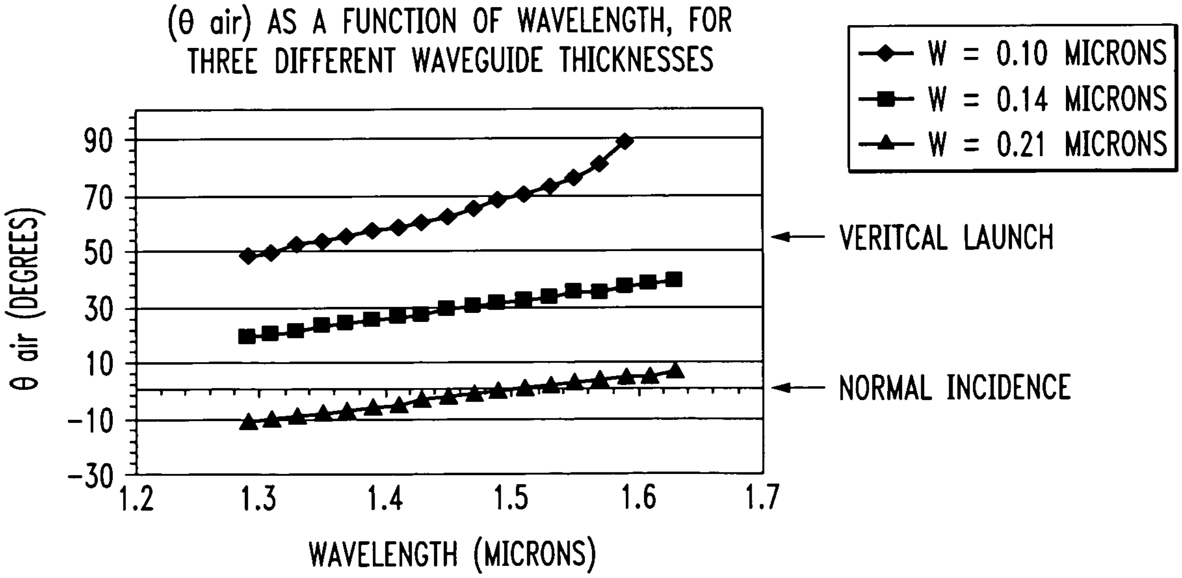

FIG. 5

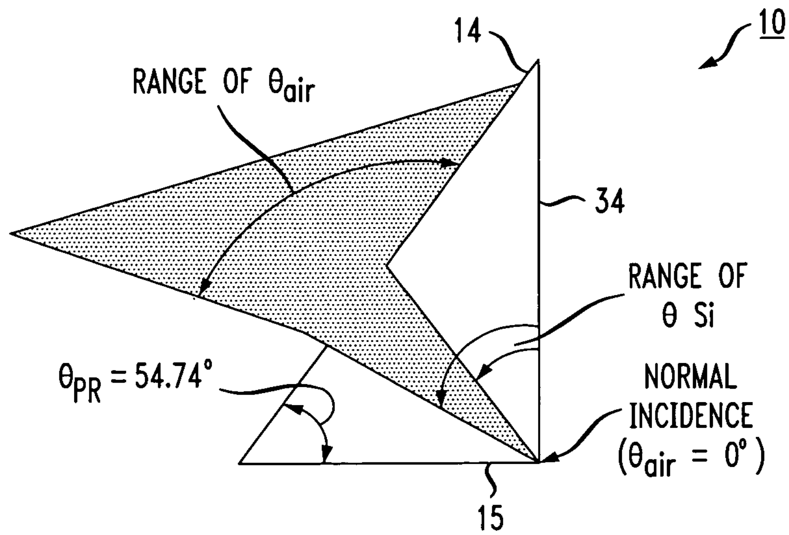
14
10
RANGE OF θ_{air}
34
RANGE OF
θ Si
$\theta_{PR} = 54.74°$
NORMAL
INCIDENCE
(θ_{air} = 0°)
15

FIG. 6

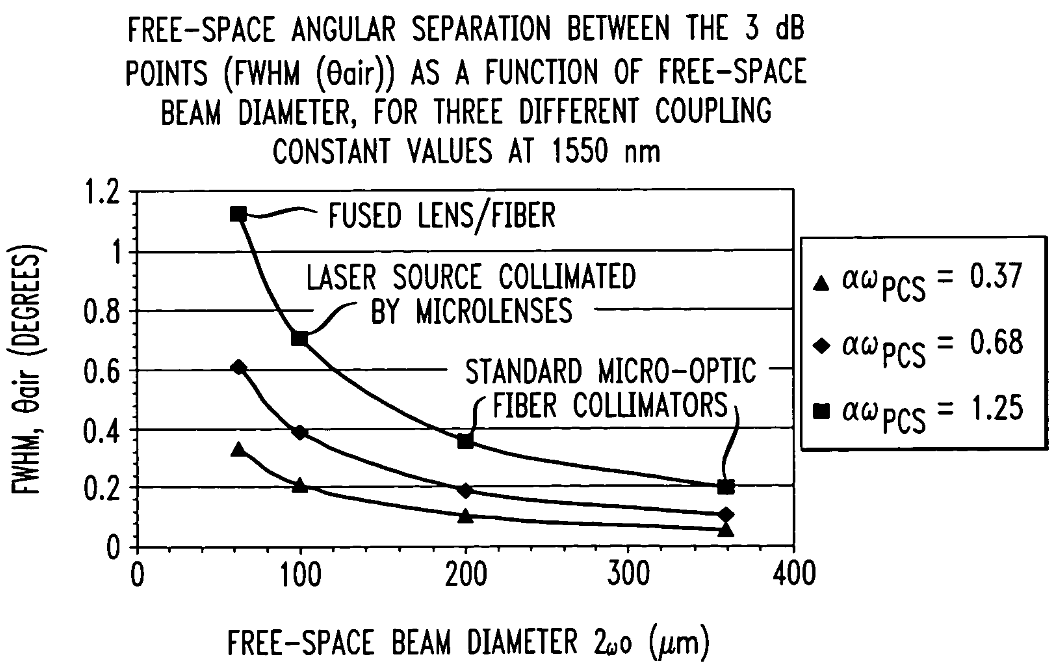
FREE-SPACE ANGULAR SEPARATION BETWEEN THE 3 dB POINTS (FWHM (θair)) AS A FUNCTION OF FREE-SPACE BEAM DIAMETER, FOR THREE DIFFERENT COUPLING CONSTANT VALUES AT 1550 nm
FUSED LENS/FIBER
LASER SOURCE COLLIMATED BY MICROLENSES
STANDARD MICRO-OPTIC FIBER COLLIMATORS
$\alpha\omega_{PCS}$ = 0.37
$\alpha\omega_{PCS}$ = 0.68
$\alpha\omega_{PCS}$ = 1.25
FWHM, θair (DEGREES)
FREE-SPACE BEAM DIAMETER 2ωo (μm)
1.2
1
0.8
0.6
0.4
0.2
0
0
100
200
300
400

FIG. 7

n = 1.45 FOR EVANESCENT LAYER

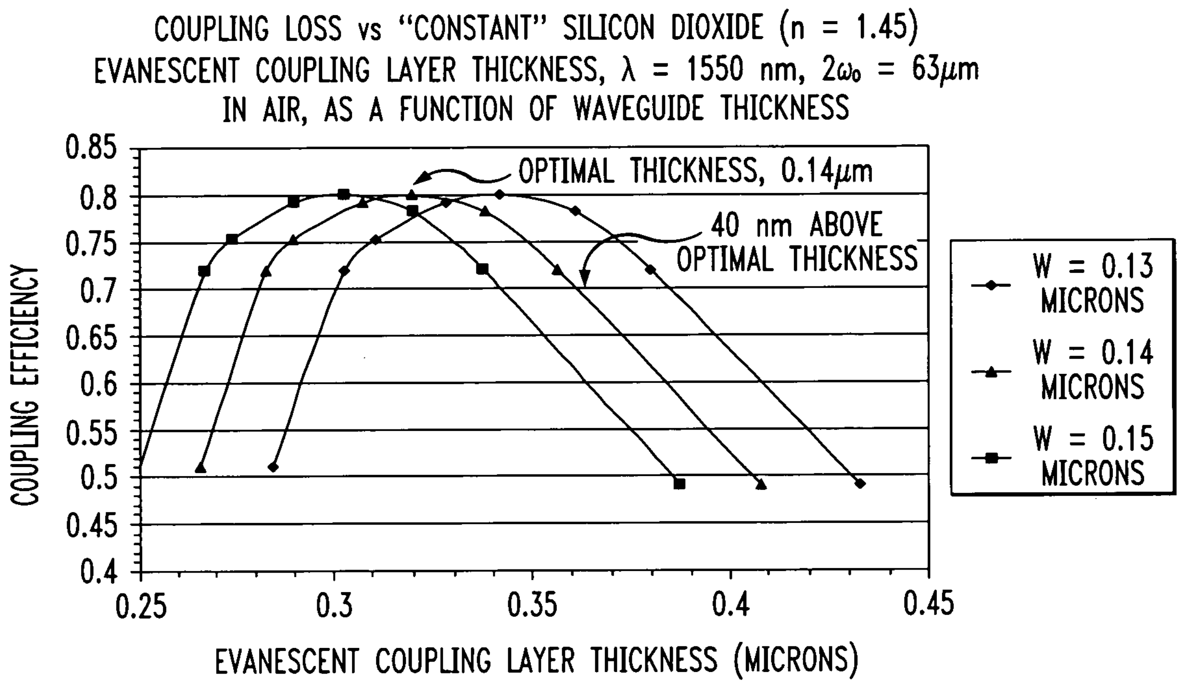

FIG. 8

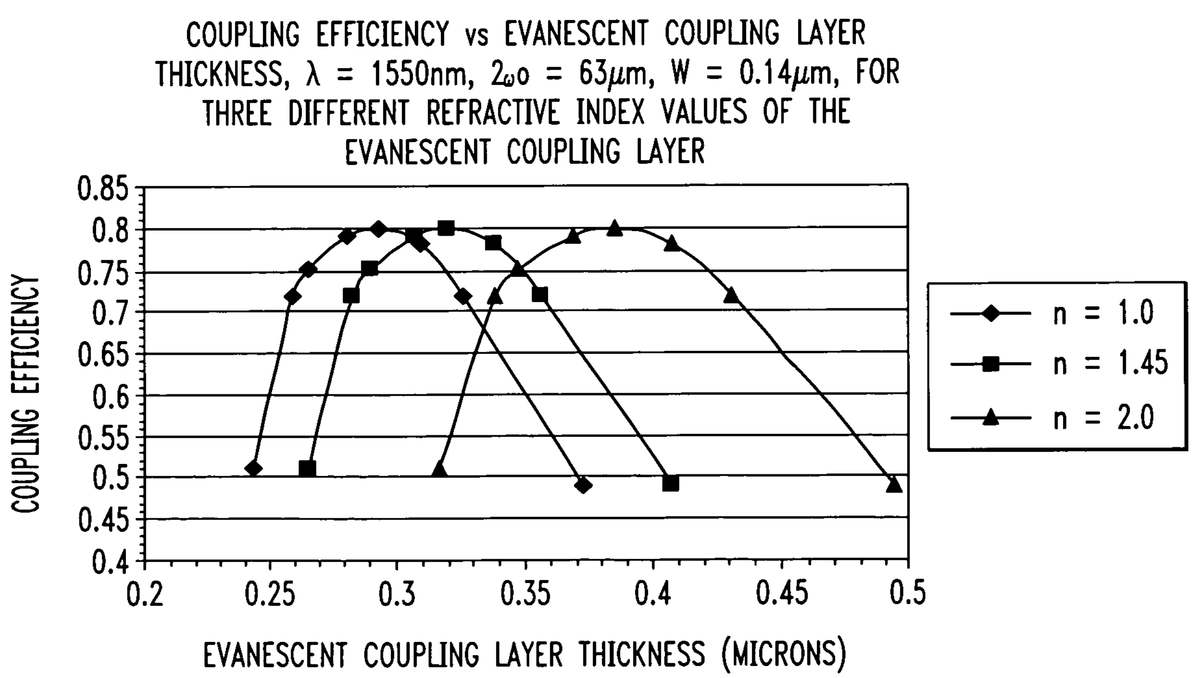

FIG. 9

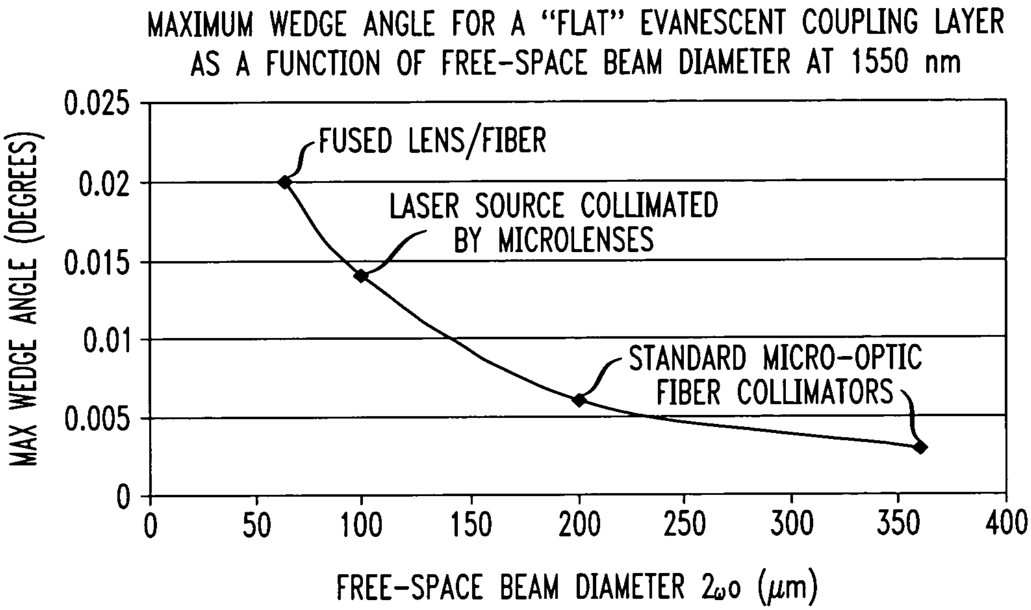
MAXIMUM WEDGE ANGLE FOR A "FLAT" EVANESCENT COUPLING LAYER AS A FUNCTION OF FREE-SPACE BEAM DIAMETER AT 1550 nm
MAX WEDGE ANGLE (DEGREES)
0.025
0.02
0.015
0.01
0.005
0
FUSED LENS/FIBER
LASER SOURCE COLLIMATED BY MICROLENSES
STANDARD MICRO-OPTIC FIBER COLLIMATORS
0
50
100
150
200
250
300
350
400
FREE-SPACE BEAM DIAMETER 2ωo (μm)

FIG. 10

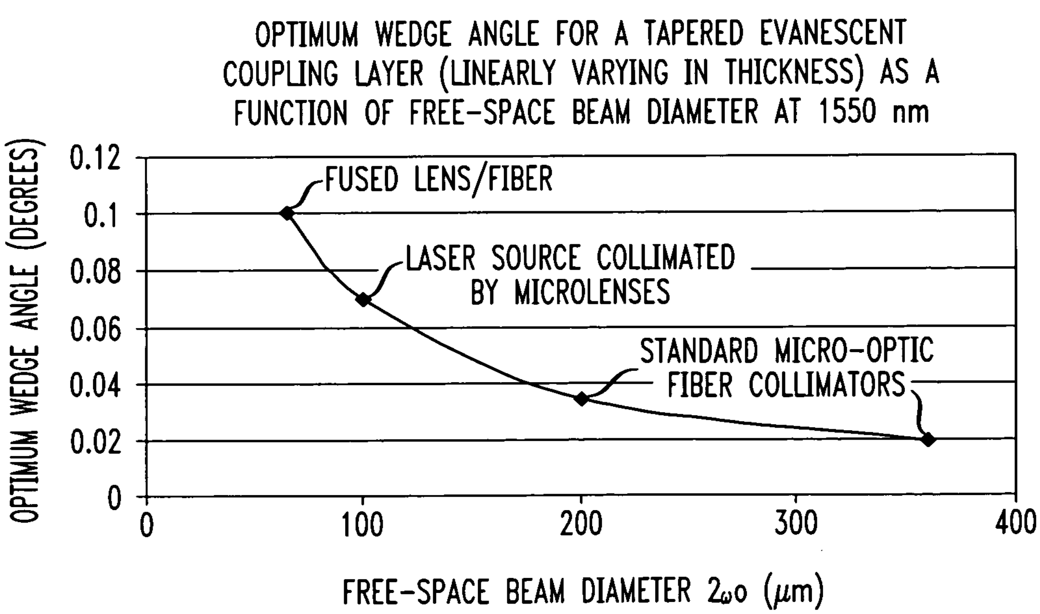
OPTIMUM WEDGE ANGLE FOR A TAPERED EVANESCENT COUPLING LAYER (LINEARLY VARYING IN THICKNESS) AS A FUNCTION OF FREE-SPACE BEAM DIAMETER AT 1550 nm
OPTIMUM WEDGE ANGLE (DEGREES)
0.12
0.1
0.08
0.06
0.04
0.02
0
FUSED LENS/FIBER
LASER SOURCE COLLIMATED BY MICROLENSES
STANDARD MICRO-OPTIC FIBER COLLIMATORS
0
100
200
300
400
FREE-SPACE BEAM DIAMETER 2ωo (μm)

FIG. 11

GRAPHS OF $2\omega_{PCS}/2\omega_o = \{1-(\sin\theta_{air}/n_{si})^2\}^{1/2}/\{\cos\theta_{air} * \cos\theta_{si}\}$

RATION OF PROJECTION OF INPUT BEAM ON PRISM COUPLING SURFACE TO FREE SPACE BEAM SIZE, AS A FUNCTION OF WAVELENGTH FOR 4 DIFFERENT WAVEGUIDE THICKNESSES OF THE EMBODIMENT SHOWN IN FIGURE 2.1, WITH θpr = 54.74 DEGREES

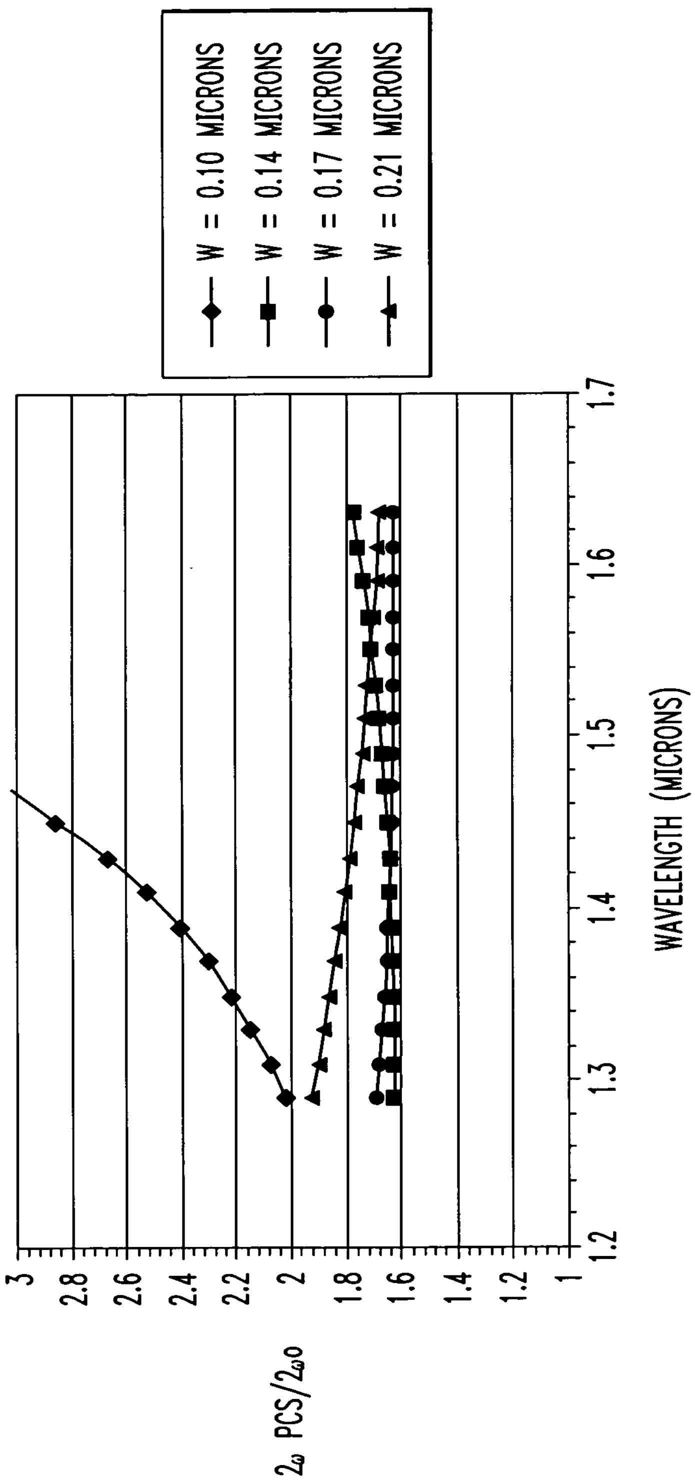

FIG. 12

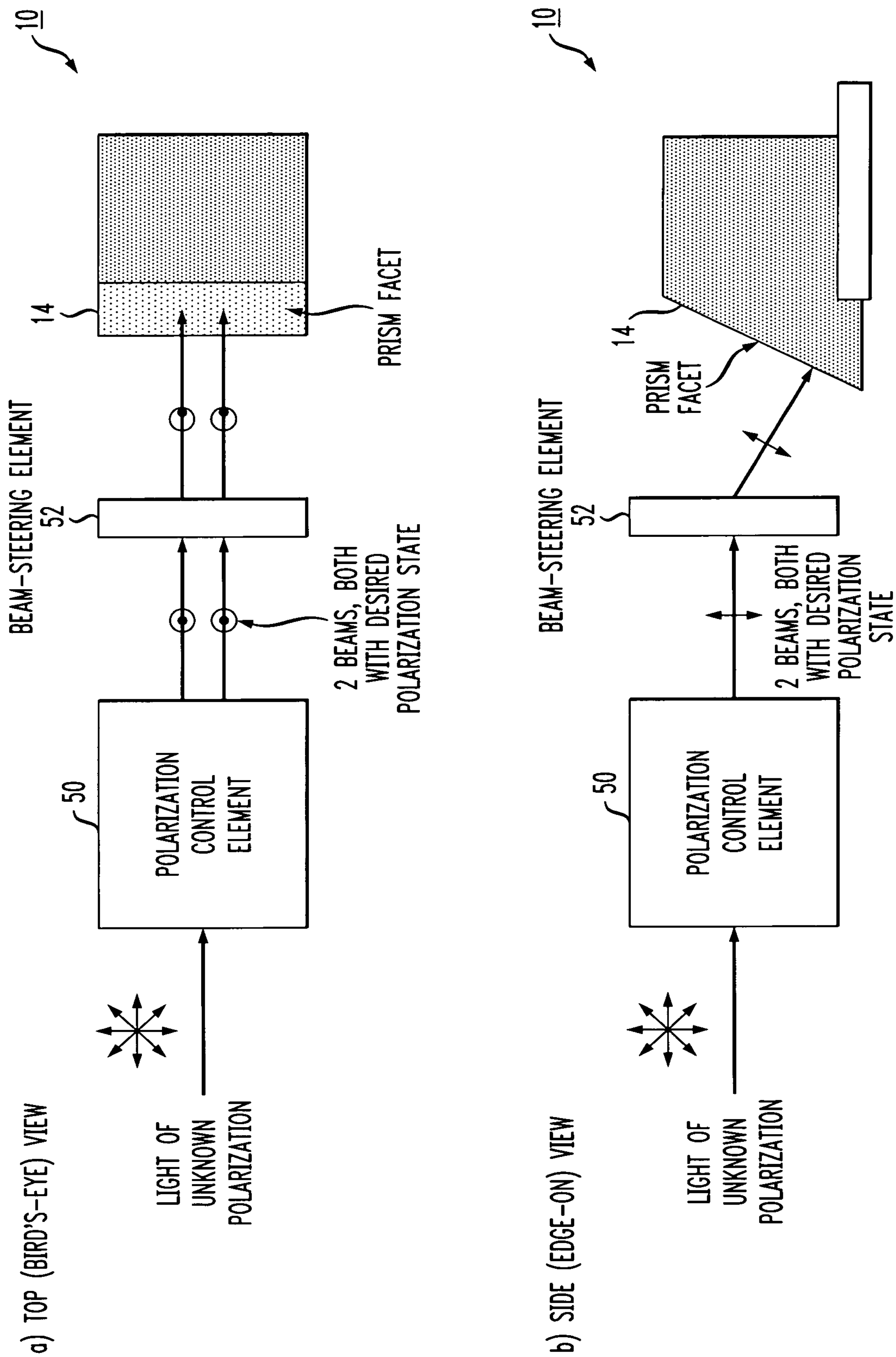
a) TOP (BIRD'S-EYE) VIEW
10
LIGHT OF UNKNOWN POLARIZATION
50
POLARIZATION CONTROL ELEMENT
2 BEAMS, BOTH WITH DESIRED POLARIZATION STATE
52
BEAM-STEERING ELEMENT
14
PRISM FACET
b) SIDE (EDGE-ON) VIEW
10
LIGHT OF UNKNOWN POLARIZATION
50
POLARIZATION CONTROL ELEMENT
2 BEAMS, BOTH WITH DESIRED POLARIZATION STATE
52
BEAM-STEERING ELEMENT
14
PRISM FACET

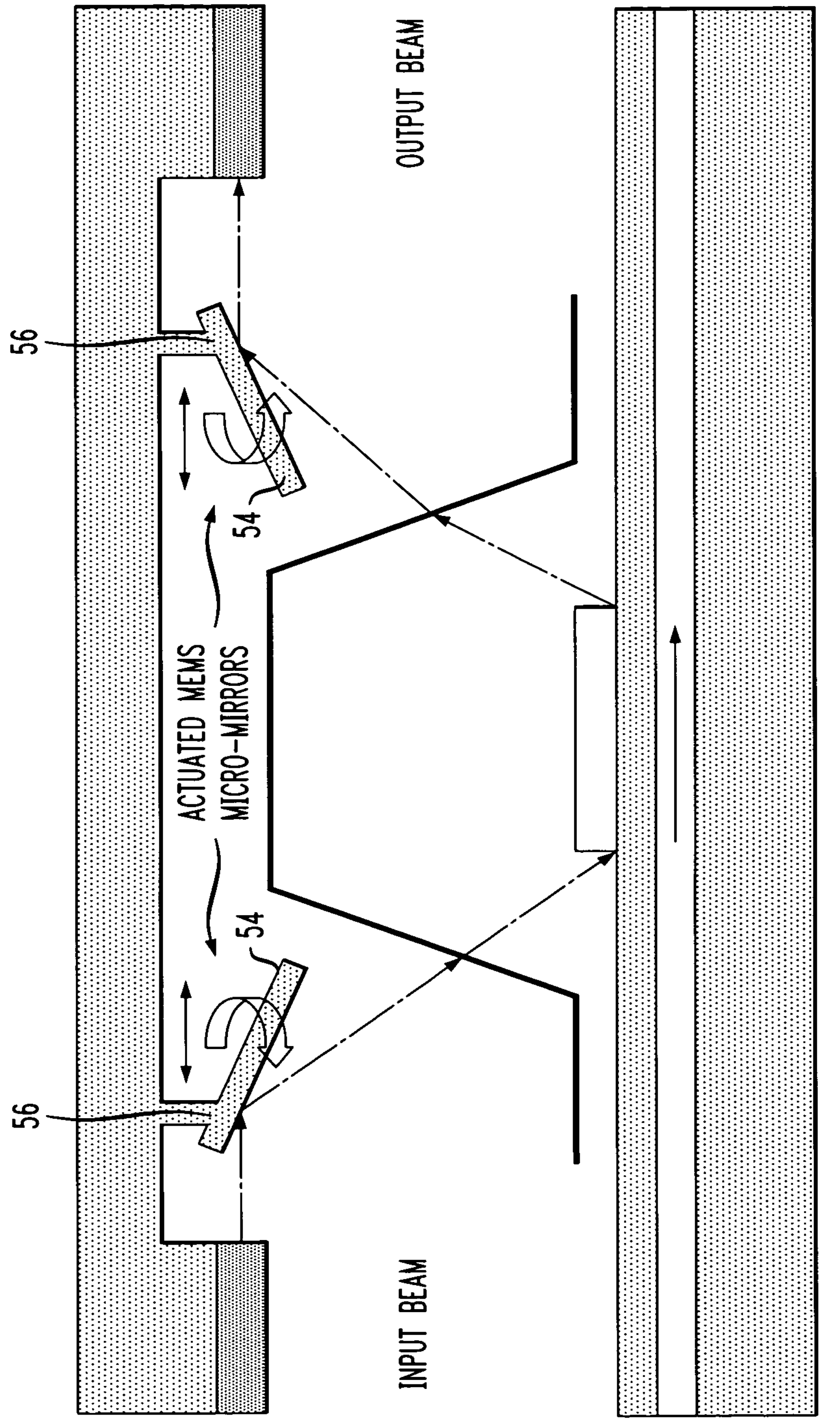
OUTPUT BEAM
56
54
ACTUATED MEMS
MICRO-MIRRORS
54
56
INPUT BEAM

FIG. 13

FIG. 14

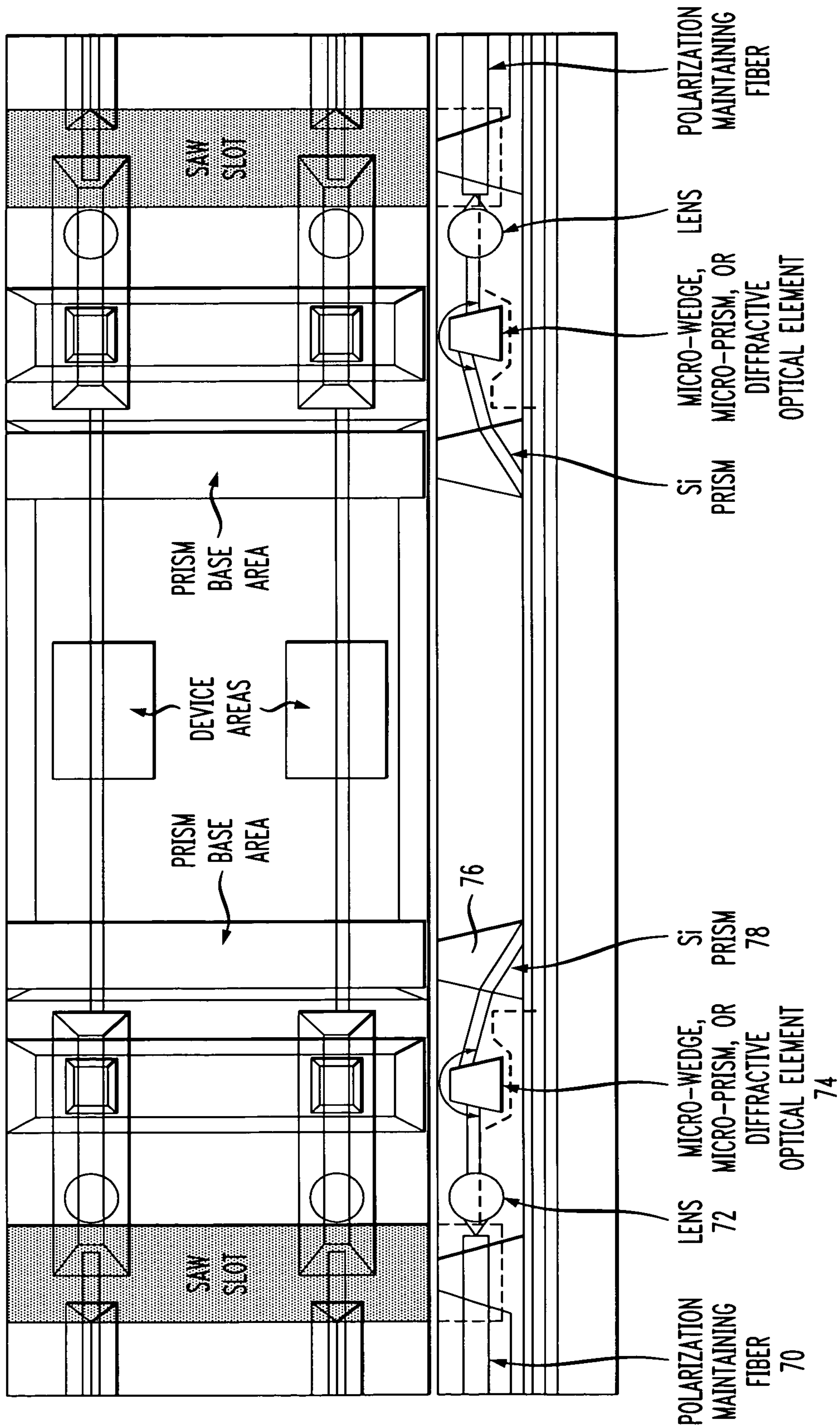
POLARIZATION MAINTAINING FIBER
LENS
MICRO-WEDGE, MICRO-PRISM, OR DIFFRACTIVE OPTICAL ELEMENT
Si PRISM
SAW SLOT
PRISM BASE AREA
DEVICE AREAS
PRISM BASE AREA
76
Si PRISM 78
MICRO-WEDGE, MICRO-PRISM, OR DIFFRACTIVE OPTICAL ELEMENT 74
LENS 72
SAW SLOT
POLARIZATION MAINTAINING FIBER 70

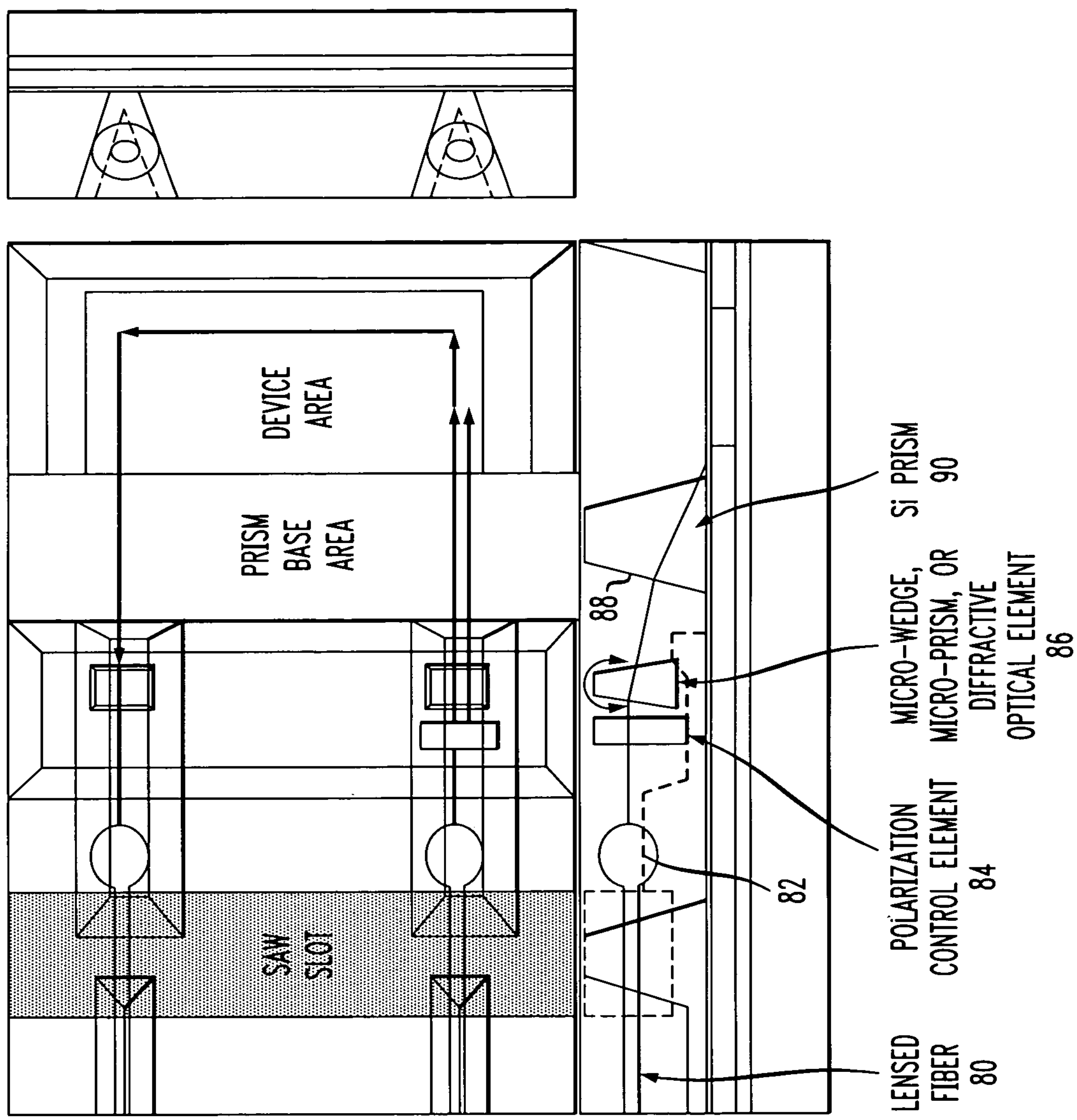
DEVICE AREA
PRISM BASE AREA
SAW SLOT
88
Si PRISM 90
MICRO-WEDGE, MICRO-PRISM, OR DIFFRACTIVE OPTICAL ELEMENT 86
82
POLARIZATION CONTROL ELEMENT 84
LENSED FIBER 80

FIG. 15

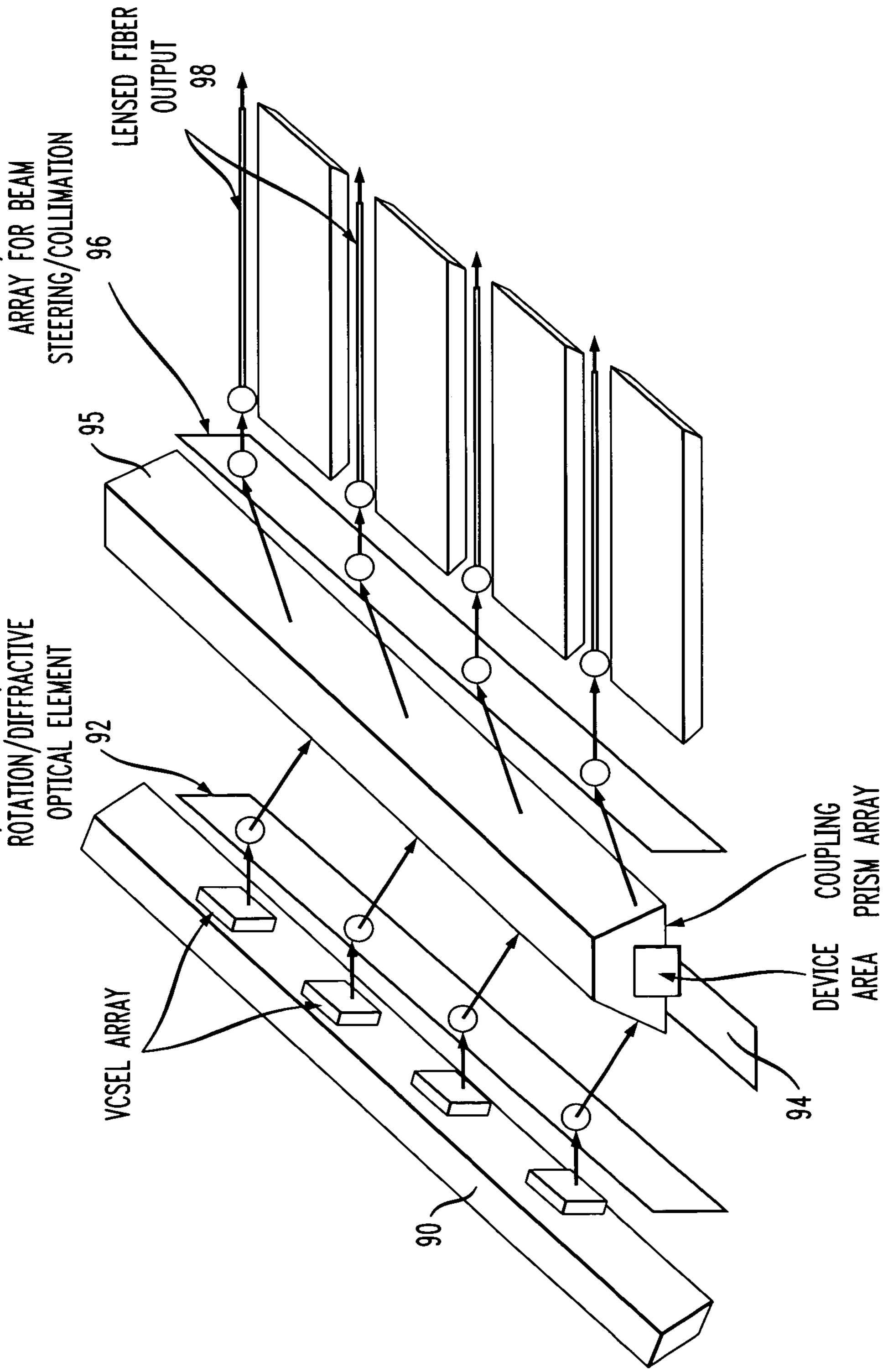
LENSED FIBER
OUTPUT
98
MICROLENS/MICROPRISM
ARRAY FOR BEAM
STEERING/COLLIMATION
96
95
MICROLENS/MICROPRISM
ARRAY FOR BEAM
STEERING/COLLIMATION/POLARIZATION
ROTATION/DIFFRACTIVE
OPTICAL ELEMENT
92
VCSEL ARRAY
90
COUPLING
PRISM ARRAY
DEVICE
AREA
94

FIG. 16

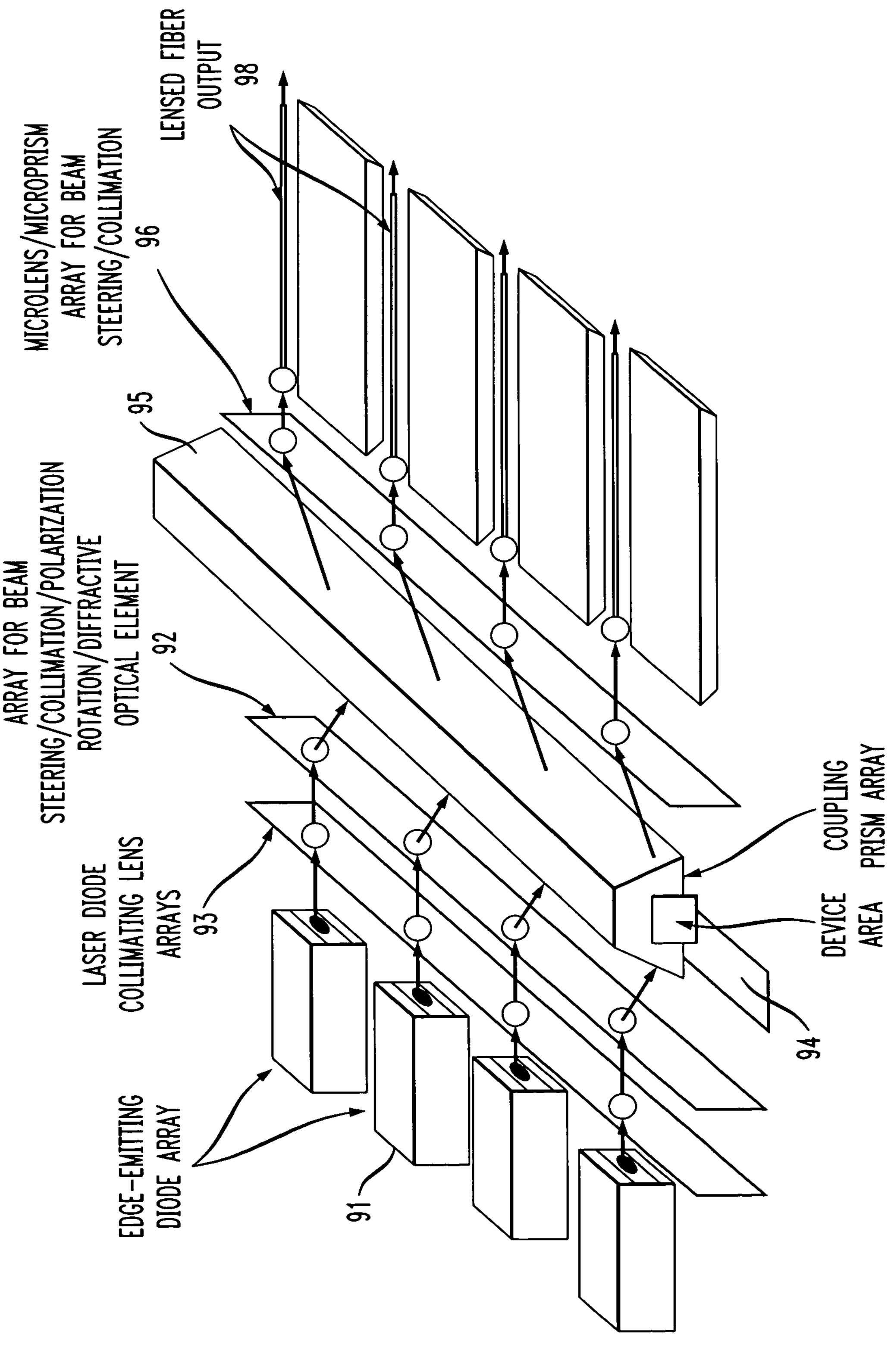
EDGE-EMITTING DIODE ARRAY
91
LASER DIODE COLLIMATING LENS ARRAYS
93
MICROLENS/MICROPRISM ARRAY FOR BEAM STEERING/COLLIMATION/POLARIZATION ROTATION/DIFFRACTIVE OPTICAL ELEMENT
92
95
MICROLENS/MICROPRISM ARRAY FOR BEAM STEERING/COLLIMATION
96
LENSED FIBER OUTPUT
98
COUPLING PRISM ARRAY
DEVICE AREA
94

FIG. 17

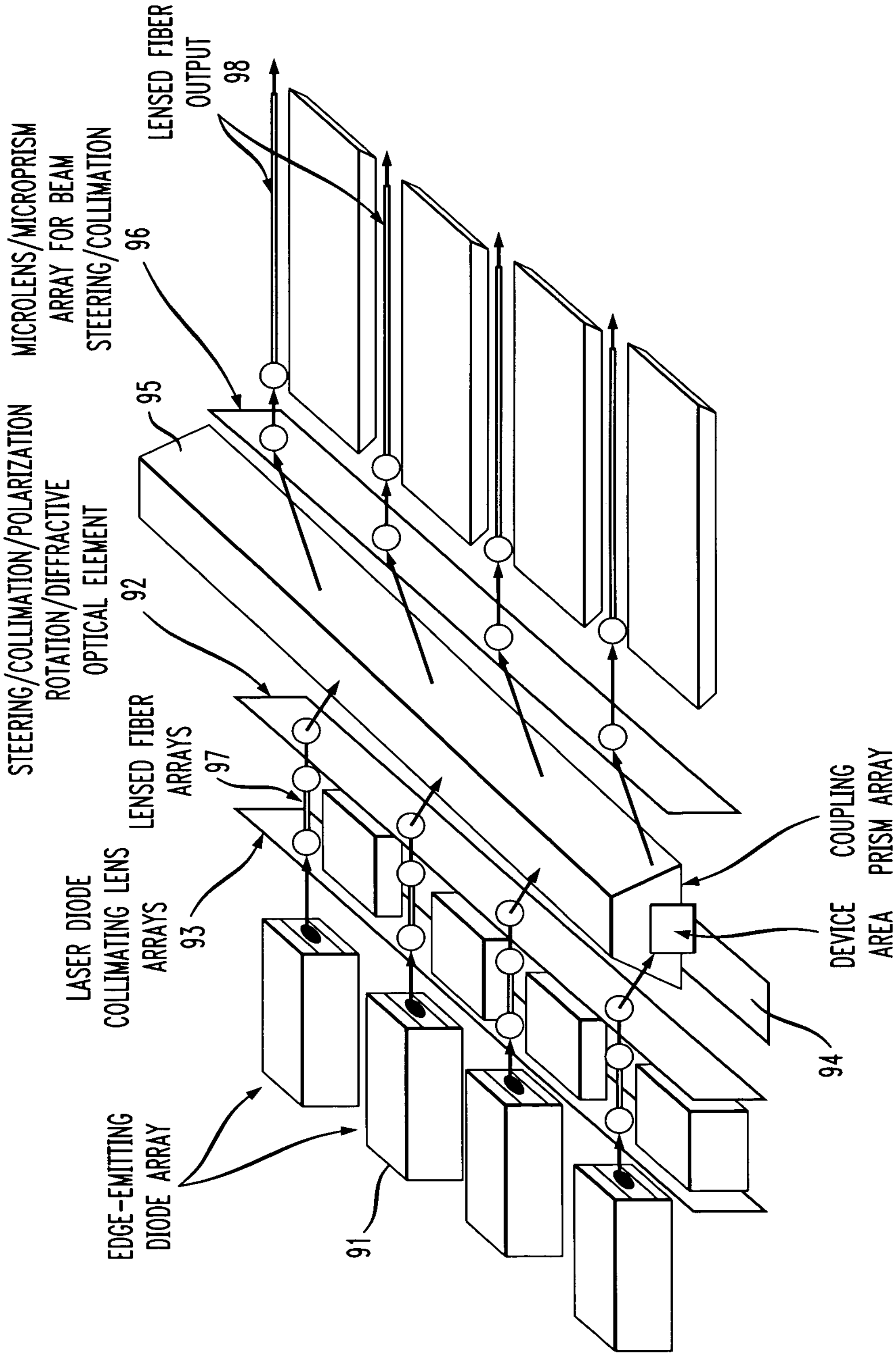
EDGE-EMITTING DIODE ARRAY
91
LASER DIODE COLLIMATING LENS ARRAYS
93
LENSED FIBER ARRAYS
97
MICROLENS/MICROPRISM ARRAY FOR BEAM STEERING/COLLIMATION/POLARIZATION ROTATION/DIFFRACTIVE OPTICAL ELEMENT
92
95
MICROLENS/MICROPRISM ARRAY FOR BEAM STEERING/COLLIMATION
96
LENSED FIBER OUTPUT
98
COUPLING PRISM ARRAY
DEVICE AREA
94

FIG. 18

FIG. 19

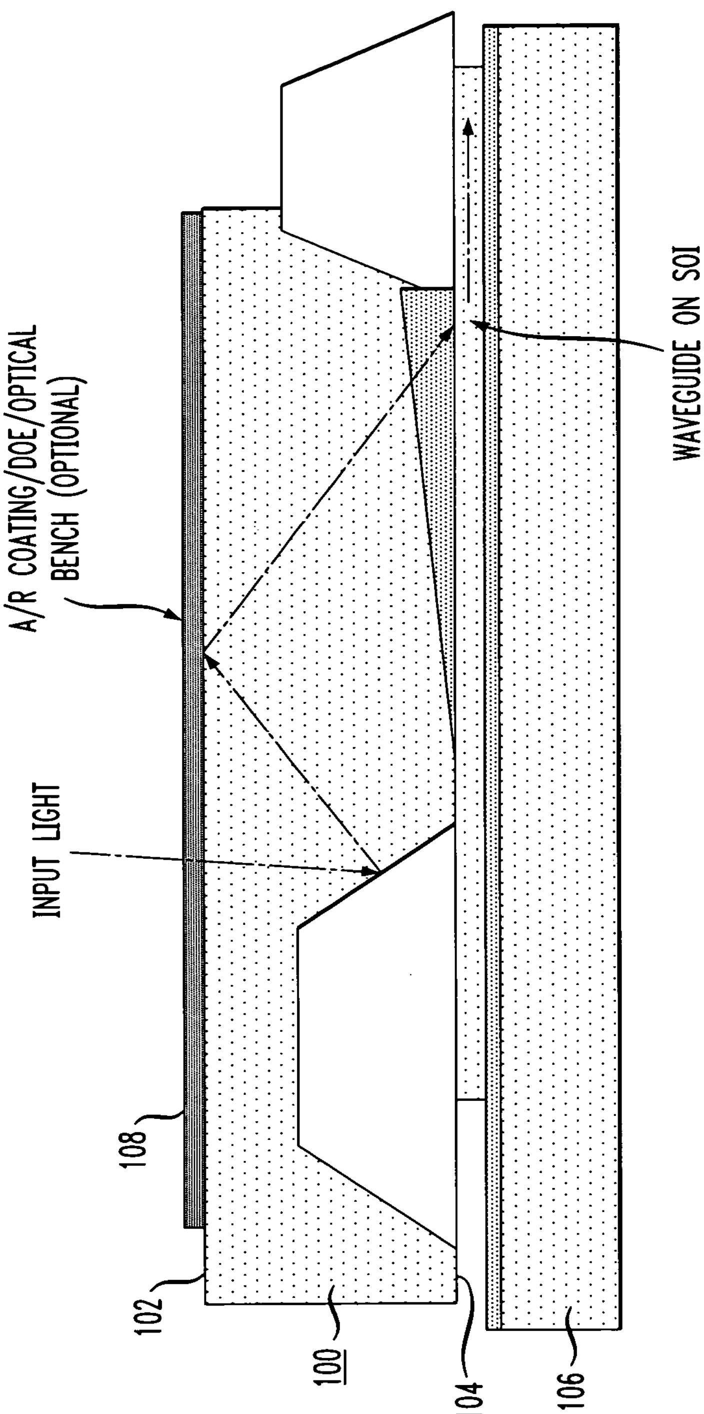
A/R COATING/DOE/OPTICAL BENCH (OPTIONAL)
INPUT LIGHT
WAVEGUIDE ON SOI
108
102
100
104
106

FIG. 20

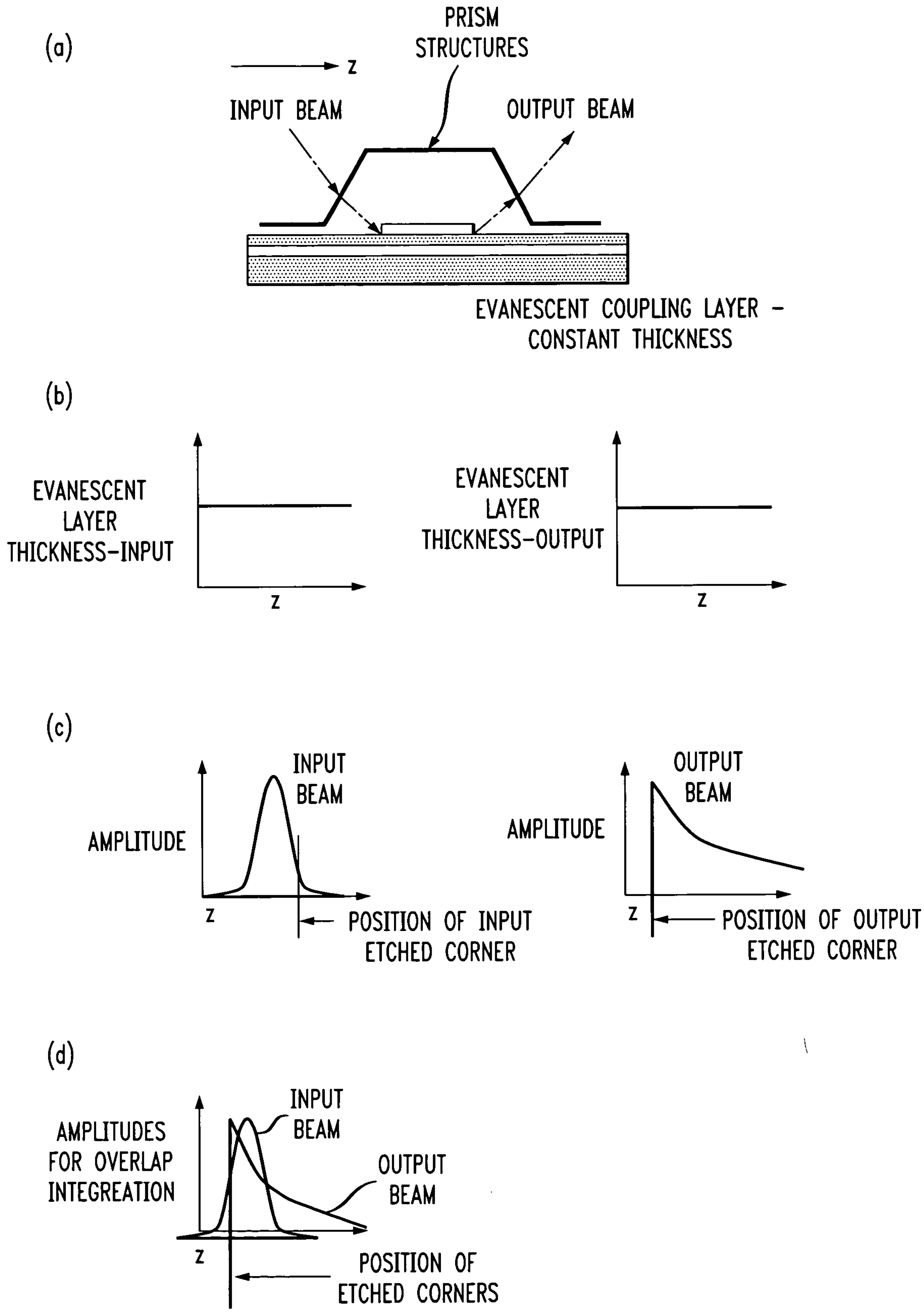
(a)
z
PRISM
STRUCTURES
INPUT BEAM
OUTPUT BEAM
EVANESCENT COUPLING LAYER -
CONSTANT THICKNESS
(b)
EVANESCENT
LAYER
THICKNESS-INPUT
z
EVANESCENT
LAYER
THICKNESS-OUTPUT
z
(c)
INPUT
BEAM
AMPLITUDE
z
POSITION OF INPUT
ETCHED CORNER
OUTPUT
BEAM
AMPLITUDE
z
POSITION OF OUTPUT
ETCHED CORNER
(d)
INPUT
BEAM
AMPLITUDES
FOR OVERLAP
INTEGRATION
OUTPUT
BEAM
z
POSITION OF
ETCHED CORNERS

FIG. 21

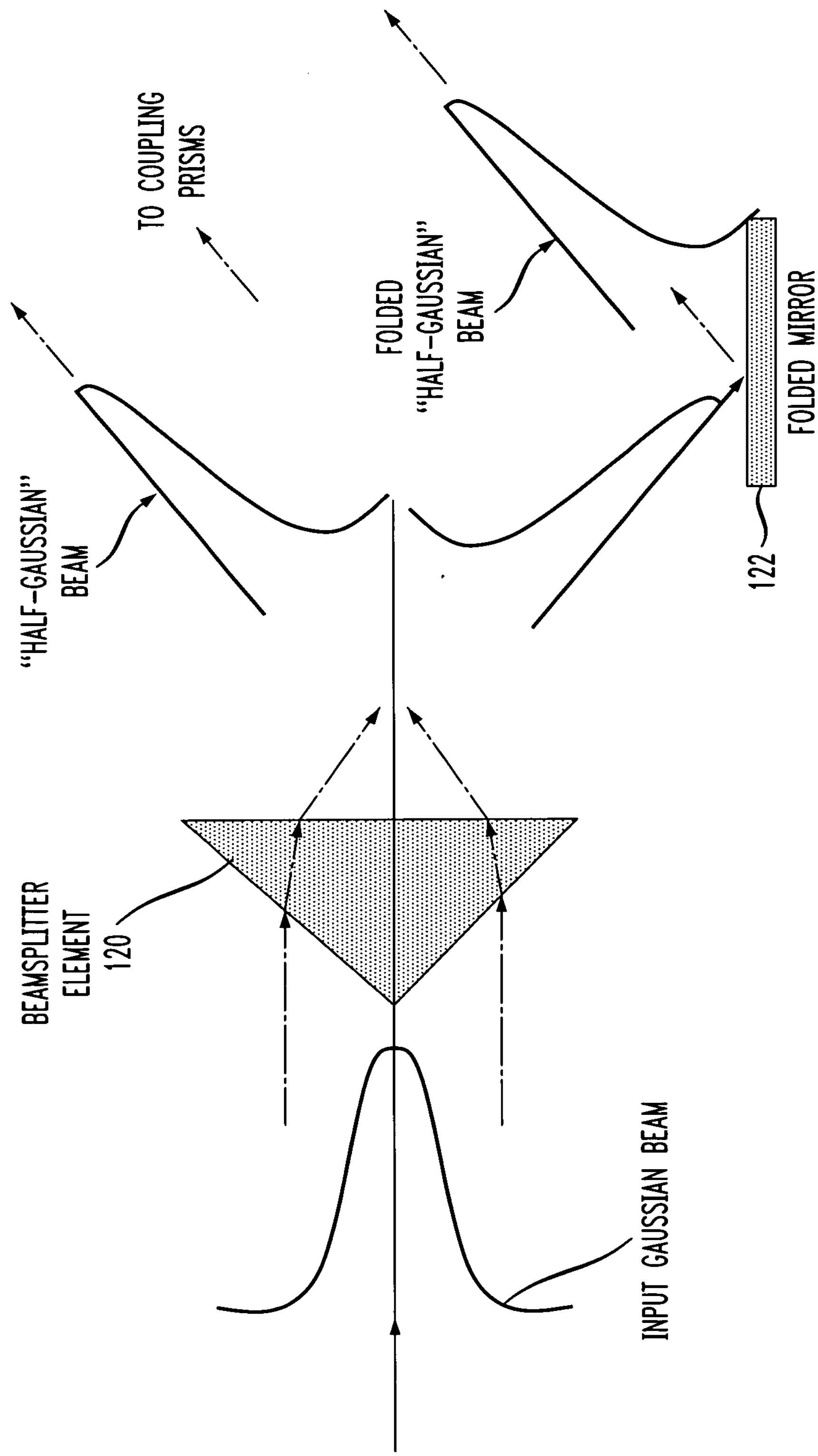
BEAMSPLITTER ELEMENT 120
"HALF-GAUSSIAN" BEAM
TO COUPLING PRISMS
FOLDED "HALF-GAUSSIAN" BEAM
FOLDED MIRROR
122
INPUT GAUSSIAN BEAM

FIG. 22

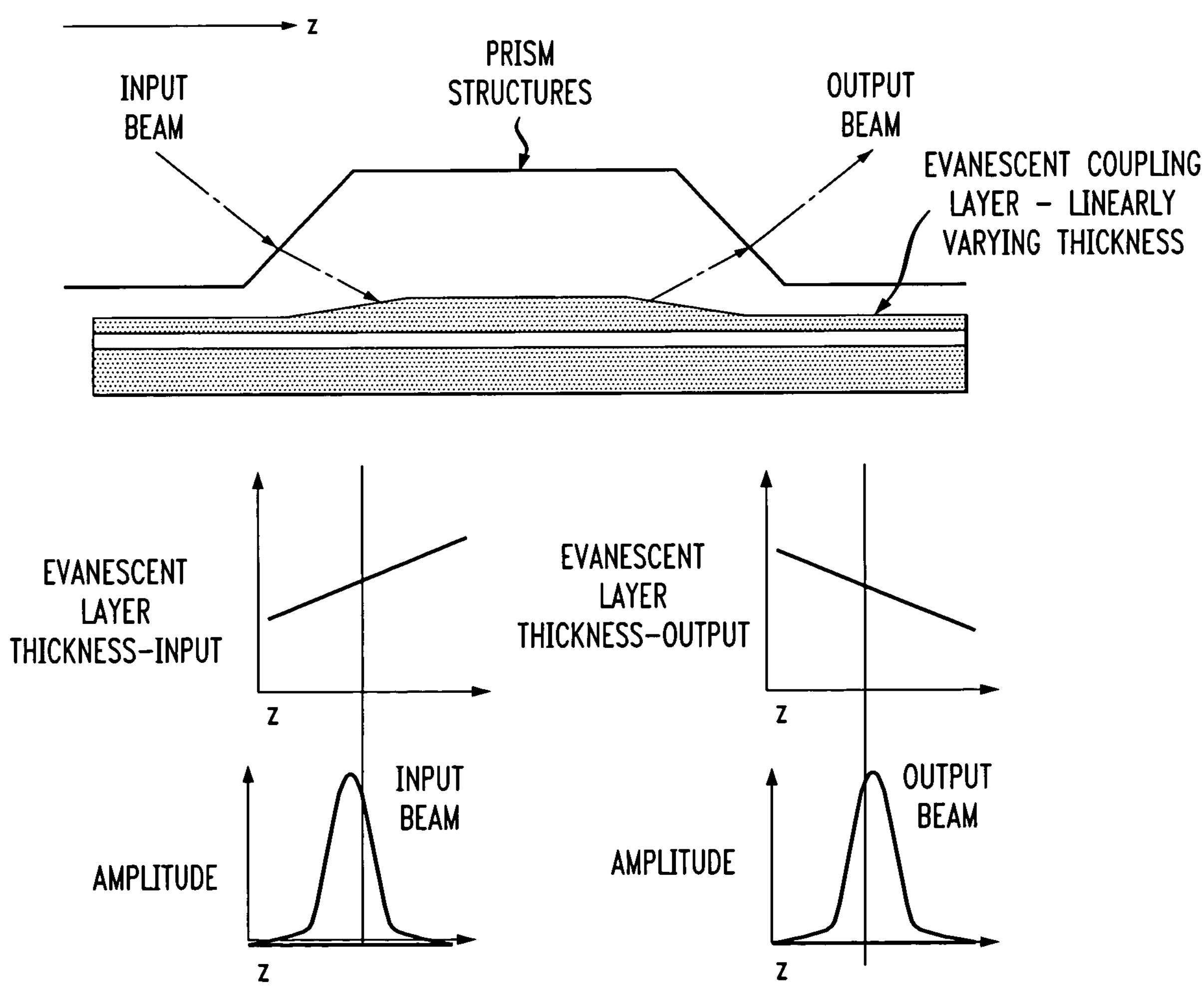
z
PRISM
STRUCTURES
INPUT
BEAM
OUTPUT
BEAM
EVANESCENT COUPLING
LAYER - LINEARLY
VARYING THICKNESS
EVANESCENT
LAYER
THICKNESS-INPUT
z
EVANESCENT
LAYER
THICKNESS-OUTPUT
z
INPUT
BEAM
AMPLITUDE
z
OUTPUT
BEAM
AMPLITUDE
z